Iranian Journal of Pharmaceutical Sciences
SPring 2008: 4(2): 127-134
www.ijps.ir

Original Article

Synthesis and Characterization of Hydroxyapatite Nanocrystals via Chemical Precipitation Technique

Hossein Eslami, Mehran Solati-Hashjin, Mohammadreza Tahriri*

Biomaterial Group, Faculty of Biomedical Engineering, Amirkabir University of Technology, Tehran, Iran

Abstract

In this study, hydroxyapatite (HA) nanocrystals have been synthesized via chemical precipitation technique. Diammonium hydrogen phosphate and calcium nitrate 4-hydrate were used as starting materials and sodium hydroxide solution was used as the agent for pH adjustment. The powder sample was evaluated by techniques such as scanning electron microscope, transmission electron microscope, Fourier transform infra-red spectroscopy, differential thermal analysis, thermal gravimetric analysis, X-ray diffraction, atomic absorption spectroscopy and EDTA titration analyses. According to the above-experimental results, it was found that hydroxyapatite nanocrystals can successfully be produced through wet precipitation method. The bulk Ca/P molar ratio of synthesized hydroxyapatite was determined as 1.71 that was higher than stoichiometric ratio (1.667) which is expected for a pure HA phase. Finally, transmission electron microscopic technique demonstrated that the crystallites of prepared powder were nanosized with a needle-like morphology.

Keywords: Hydroxyapatite; Nanocrystals; Precipitation; Synthesis.
Received: December 20, 2007; *Accepted:* March 19, 2008

1. Introduction

In recent years, significant research effort has been devoted to developing inorganic nanocrystals because of their potential application in biology, electronics, optics, transportation, and information technology. Although several approaches investigated ways of making these nanocrystals, controlling the size, shape and crystallinity and various parameters affecting the size and shape of these materials still need to be found [1].

Synthetic ceramic materials based on calcium phosphates (CaP) particularly in the composition of tricalcium phosphate [TCP: $Ca_3(PO_4)_2$] and hydroxyapatite [HA; $Ca_{10}(PO_4)_6(OH)_2$] have extensively been studied and clinically used. Biomaterials research field focus on the synthesis of these ceramics for three decades to applications in orthopedics and dentistry [2-7]. Their use is proposed because they exhibit biological affinity and activity to surrounding host tissues when implanted. Furthermore, according to the literature, calcium phosphates are widely used in medicine and oral biology due to the apatite-like structure of enamel, dentin and bones, usually called "hard tissues". To date, in spite

---

*Corresponding author: Mohammadreza Tahriri, Biomaterial Group, Faculty of Biomedical Engineering, Amirkabir University of Technology, Tehran, Iran. P.O.Box 15875-4413
Tel/Fax (+98)912-2388573
E-mail: m-tahriri@aut.ac.ir

of availability of several sophisticated characterization techniques for investigation of tooth and bone tissues, their exact composition, distribution of phases and structure remain unresolved [3]. Synthetic Ca-P preparations aim to understand the properties and physicochemical behavior of biological mineral phases found in human hard tissues because of some order of similarity among them [4]. In addition to that, these materials are also important in the study of biomineralization since they are precursors and major components of bone and teeth [8]. In order to gain insights into the complex structure found in biological mineral phases there would be required a well-defined characterization of the synthetic Ca-P, where the composition, crystallinity and nanostructure have to be properly addressed. These properties play a major role in the bioactivity of Ca-P based materials in terms of enhanced contact areas and degradation [5]. Detailed characterization indicates that an apatite layer is usually formed on the ceramic surface when implanted. This layer consists of carbonate-ion-containing apatite named "bone-like" apatite forming a bond with the human bone [2]. These ceramic materials can also be used as coating on implant to improve the biocompatibility [1, 8] and can be injected in bone with non-invasive surgical techniques [9]. Bioactivity of CaP materials is dependent on many factors during the synthesis procedure, such as precursor reagents, impurity contents, crystal size and morphology, concentration and mixture order of reagents, pH and temperature. Also, the bioactivity response of Ca-P materials will depend on thermal treatment profile for drying and sintering. These conditions are controlled by synthesis preparation parameters and consequently for each application a specific route is selected [6, 10].

In this investigation, we are reporting synthesis of HA nanocrystals by wet precipitation technique.

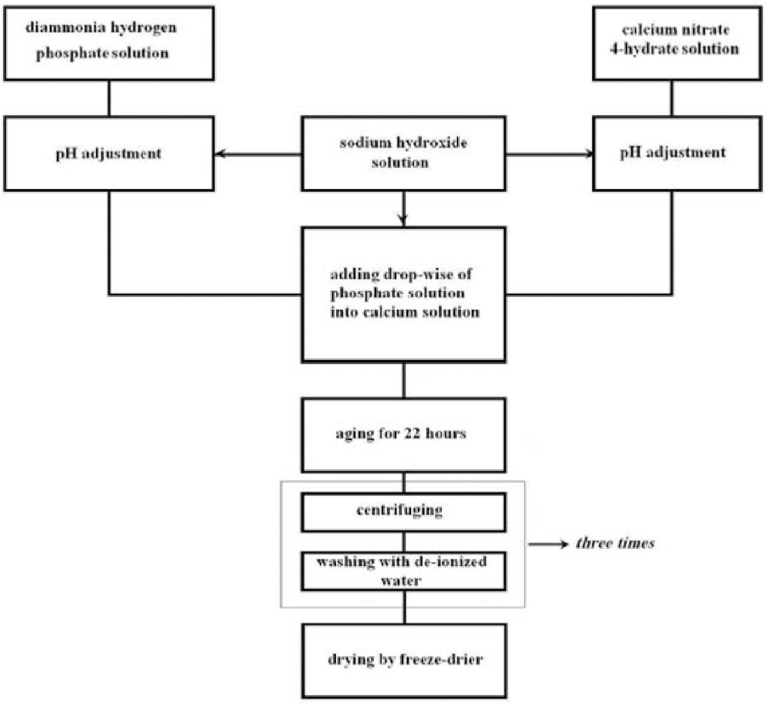

Figure 1. Flowchart for the synthesis of the hydroxyapatite powder.

2. Materials and methods

2.1.Materials and synthesis

The flowchart for the synthesis of the hydroxyapatite is illustrated in Figure 1.

Calcium nitrate 4-hydrate (36.15 g; 98%, Merck Prolabo) was dissolved in water (525 ml). Diammonium hydrogen phosphate (12 g; 99%, Merck Company) was dissolved in water (375 ml) and slowly added to the calcium nitrate solution with vigorous stirring. The solution was brought to pH 11 by addition of concentrated sodium hydroxide solution (99%, Merck). The obtained precipitation was HA. The precipitation of HA can be described by Equations (1) and /or (2) [11]:

$$10Ca^{2+}+6HPO_4^{-}+2OH^{-}\rightarrow Ca_{10}(PO_4)_6(OH)_2+6H^{+} \quad \text{Eq. (1)}$$
$$10Ca^{2+}+6H_2PO_4^{-}+2OH^{-}\rightarrow Ca_{10}(PO_4)_6(OH)_2+12H^{+} \quad \text{Eq. (2)}$$

The precipitate was aged overnight at room temperature and was thoroughly centrifuged and washed with de-ionized water. The processes of centrifuging and washing were carried out three times. The resulting powder was dried in a freeze-drier system (Alpha 1-2 LD; Germany) for 10 h. Finally, the dried powder was calcined in an electrical box furnace at 900 ºC for 1 h after heating at the rate of 5 ºC/min. in air.

2.2. Characterization

The resulting powder was analyzed by X-ray diffraction (XRD) with Siemens-Brucker D5000 diffractometer. This instrument works with voltage and current settings of 40 kV and 40 mA, respectively, and uses Cu-Kα radiation (1.540600 Å). For qualitative analysis, XRD diagrams were recorded in the interval $7^{o} \leq 2\theta \leq 60^{o}$ at scan speed of 2º /min. being the step size 0.02º and the step time 1 s. For IR analysis, the powder was dispersed into pellet of KBr and the spectra recorded by Brucker IFS 48 in the range 500 to 4000 cm^{-1}. The thermal behavior of HA was studied by simultaneously thermal analysis (STA). A thermoanalyzer (STA; Polymer Laboratories PL-STA 1640) that starting from room temperature up to 1200 ºC with the

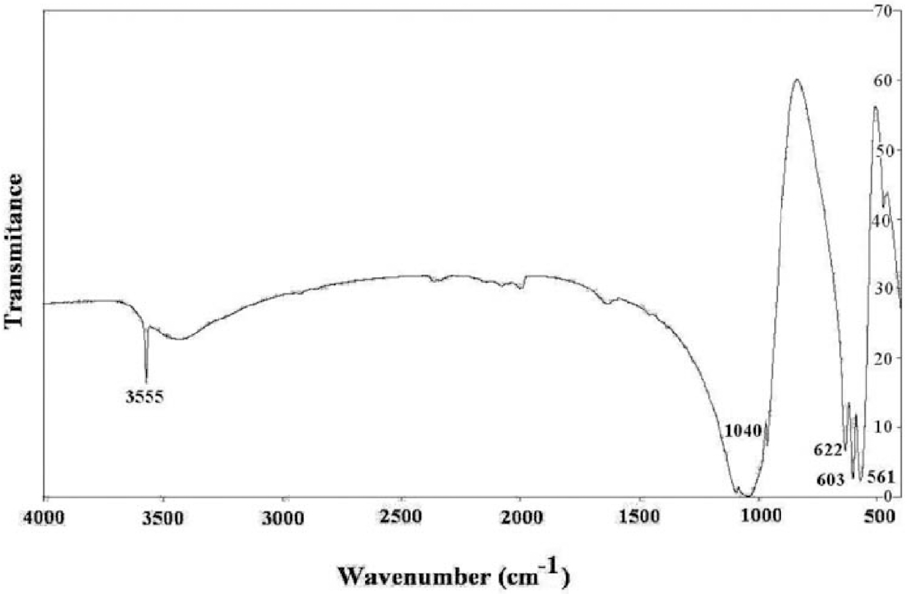

Figure 2. FT-IR spectra of the synthesized hydroxyapatite.

heating rate of 10 ºC/min. was used to record the conventional thermoanalytical curves (DTA and TGA). In order to calculate the Ca/P ratio of the precipitated powder, the amount of Ca and P were chemically analyzed by quantitative chemical analysis via EDTA titration technique and atomic absorption spectroscopy (AAS) with a Shimadzu UV-31005 instrument, respectively. Finally, transmission electron microscopy (TEM; CM200-FEG-Philips) was used for characterizing the particles. For this purpose, particles were deposited onto Cu grids, which support a carbon film. The particles were deposited onto the support grids by deposition from a dilute suspension in acetone or ethanol. The particle shapes and sizes were characterized by diffraction (amplitude) contrast and, for crystalline materials, by high resolution (phase contrast) imaging.

3. Result and discussion

3.1. FT-IR analysis

Figure 2 shows the FT-IR spectra of HA powders. The characteristic bands (listed in Table 1) exhibited in the sample spectra assigned here: (a) two bands were observed at 3555 cm^{-1} and 622 cm^{-1} due to the stretching mode of hydrogen-bonded OH^- ions and liberational mode of hydrogen-bonded OH^- ions, respectively; (b) the band at 1040 cm^{-1} arises from υ_3 PO_4, the bands at 603 cm^{-1} and 561 cm^{-1} arise from υ_4 PO_4. The FT-IR analysis showed all typical absorption characteristics of hydroxyapatite. In addition, some carbonate content also was seen (CO_3^{-2} peak around 1600 cm^{-1}), which an indication of the presence of carbonate apatite. This might have originated through the absorption of carbon dioxide from the atmosphere [12].

Therefore, according to these explanations, it is obvious that the synthesized powder is certainly hydroxyapatite.

3.2. XRD analysis

Characterization of the HA was done with XRD. The XRD analysis was performed using the X-ray diffractometer. The straight base line and the sharp peaks of the diffractogram in Figure 3 confirmed that the product was well crystallized. The XRD patterns indicated that hydroxyapatite was formed in this sample and traces of other calcium phosphate impurities were not detected by this technique.

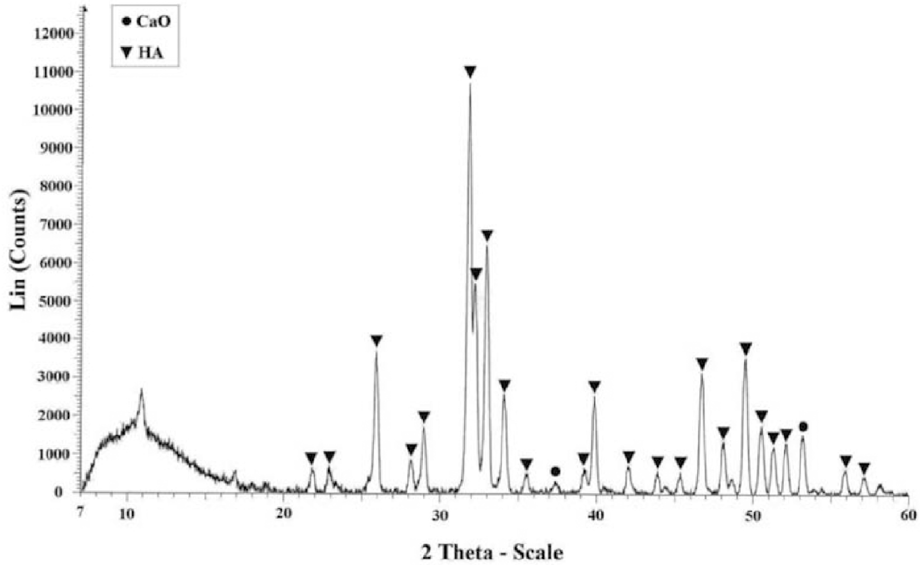

Figure 3. XRD pattern of the synthesized hydroxyapatite.

Table 1. Infrared assigned for the synthesized hydroxyapatite powder.

Infrared frequency (cm^{-1})	Assignment
561	PO_4 bend υ_4
622	OH structural
1040	PO_4 bend υ_3
3555	OH structural

Table 2. Ca and P content in the synthesized hydroxyapatite powder and Ca/P ratio.

Element	Measured content (wt %)	Ca/P ratio
Ca	38.63	1.71
P	17.48	

This can also be seen in this figure, secondary phase CaO (calcium oxide) was observed.

The intensity of (200) lattice plan of CaO on the XRD pattern of HA powder was used as a direct indicator of its purity as in the Afshar *et al.* [10] research. The ratio of the peak intensities on the XRD pattern of CaO/HA ($I_{(200)}CaO/I_{(002)}HA$), was calculated. The amounts of ($I_{(200)}CaO/I_{(002)}HA$) on sample was about 0.08. It is mentionable that, the CaO presence does not grant HA smaller biocompatibility [13]. The control of synthesis parameters commands the developing of HA purity and other phases content in bioceramics [13].

3.3. DTA and TGA analysis

The DTA and TGA (STA: Simultaneous thermal analysis) curves for the hydroxyapatite powder are illustrated in Figure 4. The first endothermic region range from 90 to 295 ºC with a peak at about 250 ºC, which corresponds to the dehydration of the precipitating complex and the loss of physically adsorbed water molecules of the HA powder. The weight loss in this region is 16%. With increasing temperature from 295 to 1200 ºC no peak has been observed, except a weight loss of 6% is observed at the TGA curve in the temperature range which is assumed to be the result of gradual dehydroxylation of HA powder. This can be explained by Equation (3) reaction [14]:

$$Ca_{10}(PO_4)_6(OH)_2 \rightarrow Ca_{10}(PO_4)_6(OH)_{2-2x}O_x\square_x + xH_2O \qquad \text{Eq. (3)}$$

3.4. Elemental analysis

The result of measurement of elemental composition (Ca and P content) and Ca/P molar ratio are summarized in Table 2. The bulk Ca/P molar ratio was determined as 1.71. The measured Ca/P ratio for this produced powder was higher than stoichiometric ratio (1.667) expected for a pure HA phase that can

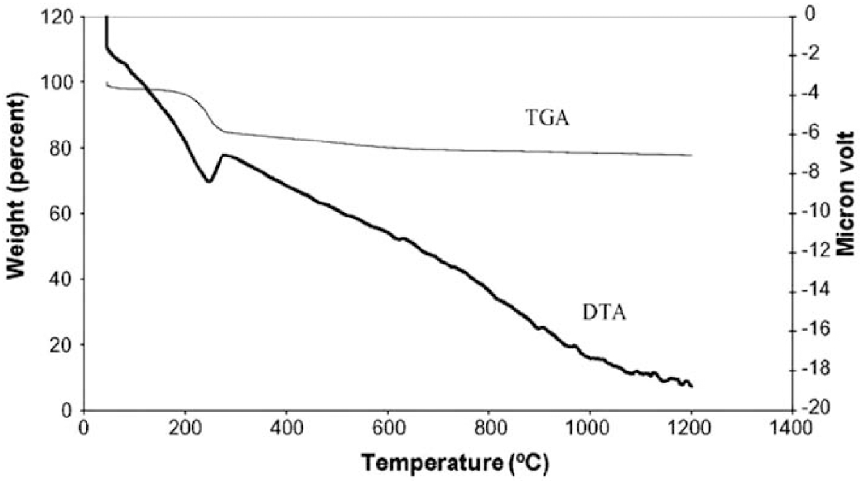

Figure 4. DTA and TGA traces of the hydroxyapatite powder.

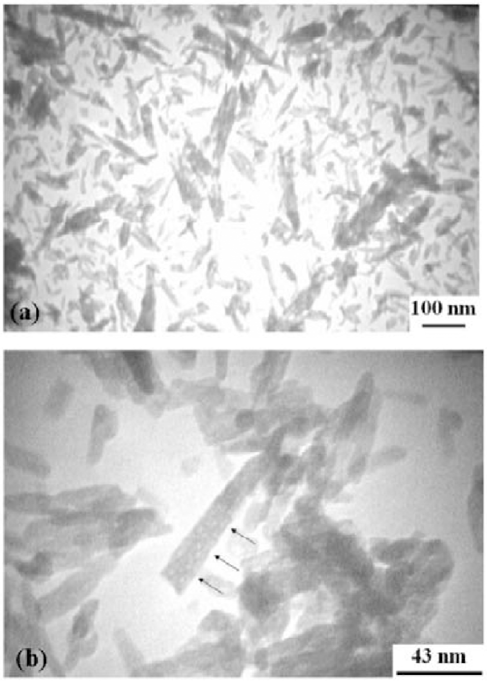

Figure 5. TEM micrographs of hydroxyapatite powder in (a) low magnification, and (b) high magnification.

arise from two matters: (a) local presence of carbonate apatite in which the Ca/P ratio can be as high as 3.33 [15] or (b) presence of impurities such as CaO. According to the XRD patterns that showed existence of small amounts of CaO phase, the second matter is much more reasonable.

3.5. TEM observations

TEM was used to examine and estimate of HA crystallites. TEM micrograph of the hydroxyapatite powder is shown in Figure 5. The microstructure of HA particles is observed to be almost like a needle, needle with a mean crystallite size of 14±5 nm in diameter and about 47±10 nm in length. As it is seen in Figure 5(b), nanoparticles indicated by arrow-head, is containing some fine holes in their intrastructure. These holes are fundamentally some structural defects that can be related to the kind of synthesis of them. Since, synthesis of HA was carried out in alkaline environment (pH was about 11), so, there are some high corrosive hydroxyl groups in the synthesis reactor which they cause the defects in the structure.

4. Conclusions

In conclusion, HA was synthesized by precipitation method as a wet chemical technique. Synthesized HA powder has been characterized on a macroscopic level by XRD, FTIR, DTA, TGA and chemical analysis (AAS and EDTA titration technique), while TEM has provided detailed information at the microscopic (individual grain) level. This technique has shown that the HA sample prepared in solution was nearly pure HA. Only low levels of specific impurities were detected.

References

[1] Eslami H, Solati-Hashjin M, Tahriri M. Synthesis and characterization of nanocrystalline fluorinated hydroxyapatite powder by a modified wet-chemical process. *J Ceram Process Res* 2008; 9: 224-9.

[2] Jones F. Teeth and bones: Applications of surface science to dental materials and related biomaterials. *Surf Sci Rep* 2001; 42: 75-205.

[3] Kikuchi M, Itoh S, Ichinose S, Shinomiya K, Tanaka J. Self-organization mechanism in a bone-like hydroxyapatite/collagen nanocomposite synthesized *in vitro* and its biological reaction *in vivo*. *Biomaterials* 2001; 22: 1705-11.

[4] Schnettler R, Alt V, Dingeldein E, Pfefferle HJ, Kilian O, Meyer C, Heiss C, Wenisch S. Bone ingrowth in bFGF-coated hydroxyapatite ceramic implants. *Biomaterials* 2003; 24: 4603-8.

[5] Liou SC, Chen SY, Liu DM. Synthesis and characterization of needlelike apatitic nanocomposite with controlled aspect ratios. *Biomaterials* 2003; 24: 3981-8.

[6] Mavropoulos E, Rossi AM, Rocha NCC, Soares GA, Moreira JC, Moure GT. Dissolution of calcium-deficient hydroxyapatite synthesized at different conditions. *Mater Charact* 2003; 5578:1-5.

[7] Li Y, Klein CPAT. Change and phase transition of need-like nonstochiometric apatite crystals. *J Mater Sci Mater Med* 1994; 5: 263-8.

[8] Fatehi K, Moztarzadeh F, Soalti-Hashjin M, Tahriri M, Rezvannia M, Ravarian R. *In vitro*

biomimetic deposition of apatite on alkaline and heat treated Ti6A14V alloy surface. *Bull Mat Sci* 2008; 31; 101-8.

[9] Weiss P, Obadia L, Magne D, Bourges X, Rau C, Weitkamp T, Khairoun I, Bouler JM, Chappard D, Gauthier O, Daculsi G. Synchrotron X-ray micro-tomography (on a micron scale) provides three-dimensional imaging representation of bone ingrowth in calcium phosphate biomaterials. *Biomaterials* 2203; 24: 4591-601.

[10] Afshar A, Ghorbani M, Ehsani N, Saeri MR, Sorrell CC. Some important factors in the wet precipitation process of hydroxyapatite. *Mater Design* 2003; 24: 197-202.

[11] Morales JG, Burgues JT, Boix T, Fraile J, Clemente RR. Precipitation of stoichiometric hydroxyapatite by a continuous method. *Cryst Res Technol* 2001; 36:15-26.

[12] Komath M, Varma HK. Development of a fully injectable calcium phosphate cement for orthopedic and dental applications. *Bull Mater Sci* 2003; 4: 415-22.

[13] Rameshbabu N, Kumar TSS, Rao KP. Synthesis of nanocrystalline fluorinated hydroxyapatite by microwave processing and its *in vitro* dissolution study. *Bull Mater Sci* 2006; 29: 611-5.

[14] Murray MGS, Wang J, Pontoon CB, Marquis PM. An improvement in processing of hydroxyapatite ceramics. *J Mater Sci* 1995; 30: 3061-74.

[15] Wei M, Evans JH, Bostrom T, Grondahl L. Synthesis and characterization of hydroxyapatite, fluoride-substituted hydroxyapatite and fluorapatite. *J Mater Sci Mater Med* 2003; 14: 311-20.